molecular pharmaceutics

Article

Cite This: Mol. Pharmaceutics 2019, 16, 2557−2568

pubs.acs.org/molecularpharmaceutics

Electrospinning Optimization of Eudragit E PO with and without Chlorpheniramine Maleate Using a Design of Experiment Approach

Hend E. Abdelhakim,[†] Alastair Coupe,[‡] Catherine Tuleu,[†] Mohan Edirisinghe,[§] and Duncan Q. M. Craig*[,†]

[†]School of Pharmacy, University College London (UCL), 29-39 Brunswick Square, London WC1N 1AX, U.K.

[‡]Pfizer Limited, Global R&D, Discovery Park, Ramsgate Road, Sandwich, Kent CT13 9ND, U.K.

[§]Department of Mechanical Engineering, UCL, Torrington Place, London WC1E 7JE, U.K.

ABSTRACT: Electrospinning is increasingly becoming a viable means of producing drug delivery vehicles for oral delivery, particularly as issues of manufacturing scalability are being addressed. In this study, electrospinning is explored as a taste-masking manufacturing technology for bitter drugs. The taste-masking polymer Eudragit E PO (E-EPO) was electrospun, guided by a quality by design approach. Using a design of experiment, factors influencing the production of smooth fibers were investigated. Polymer concentration, solvent composition, applied voltage, flow rate, and gap distance were the parameters examined. Of these, polymer concentration was shown to be the only statistically significant factor within the ranges studied (p-value = 0.0042). As the concentration increased, smoother fibers were formed, coupled with an increase in fiber diameter. E-EPO (35% w/v) was identified as the optimum concentration for smooth fiber production. The optimized processing conditions identified were a gap distance of 175 mm, an applied voltage of between 15 and 20 kV, and a flow rate of 1 mL/h. Using this knowledge, the production optimization of electrospun E-EPO with chlorpheniramine maleate (CPM), a bitter antihistamine drug, was explored. The addition of CPM in drug loads of 1:6 up to 1:10 CPM/E-EPO yielded smooth fibers that were electrospun under conditions similar to placebo fibers. Solid-state characterization showed CPM to be molecularly dispersed in E-EPO. An electronic tasting system, or E-tongue, indicated good taste-masking performance as compared to the equivalent physical mixtures. This study therefore describes a means of producing, optimizing, and assessing the performance of electrospun taste-masked fibers as a novel approach to the formulation of CPM and potentially other bitter drug substances.

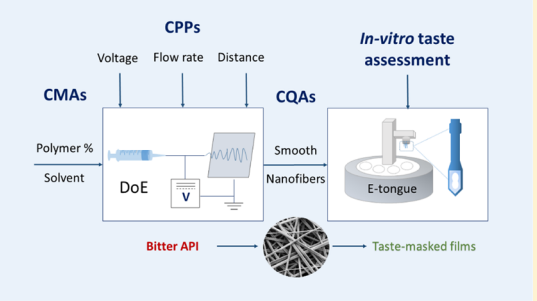

KEYWORDS: *electrospinning, taste-masking, E-tongue, Eudragit E PO, chlorpheniramine maleate, DoE*

1. INTRODUCTION

Electrospinning is based on the ultrafast removal of solvents from a fluid mixture to form solid micro- and nanofibers.[1] The method utilizes a high-voltage electric field to form a continuous jet of liquid that subsequently dries and deposits on a collector plate as the fibrous material. The applications of this technology include filtration, production of protective clothing, tissue engineering, and more recently drug delivery.[2] In the therapeutics arena, electrospun fibers are promising candidates for drug delivery owing to their high surface area to volume ratio for release, their structural flexibility, and their ability to encapsulate high drug loadings in polymeric matrices, the polymers allowing a range of performance functions in the body.[3] One such recent application of electrospinning is as an approach to taste-masking for bitter drugs.[3−7] Poor palatability of medicines is one of the main compliance barriers within the pediatric population, making most liquids unsuitable, and yet large coated solid dosage forms cannot be swallowed by children. By using taste-masking polymers, bitter drugs can be encapsulated in a form that can be both palatable and easy to swallow. Electrospun fibers can then be formulated into age appropriate dosage forms such as oral films or mini-tablets.[3,6,8] While systems such as microspheres have been extensively studied, the use of nanofibers is a relatively new approach and little is known with regard to production optimization, particularly concerning the effects of drug addition on fiber characteristics and the associated taste-masking performance.

To develop electrospinning within the pharmaceutical field, it is necessary to thoroughly explore the spinning properties of polymers relevant to therapeutic use while also being mindful of the need for therapeutic, as well as production, performance. Relatively recently, the understanding of scalability of electrospinning has increased very considerably, thus opening up the potential for viable oral delivery, which requires high volume manufacture.[9] However, by the same token, the use of materials

Received: February 6, 2019
Revised: April 18, 2019
Accepted: April 25, 2019
Published: April 25, 2019

DOI: 10.1021/acs.molpharmaceut.9b00159
Mol. Pharmaceutics 2019, 16, 2557−2568

typically associated with oral delivery have not yet been extensively studied as electrospinning materials. The challenge therefore lies in the need to consider:

(a) Spinnability of pharmaceutical grade materials for which there is little or no precedent
(b) Formation optimization for those materials, particularly being mindful of the need to consider the effects of drug addition
(c) Development of suitable markers that allow reasonable prediction of biological performance at a preclinical stage.

In this study, we explore the production of Eudragit E PO (E-EPO) fibers, a taste-masking polymer, both alone and incorporating chlorpheniramine maleate (CPM), an antihistamine used by children for conditions such as urticaria, hay fever, and relief of itching associated with chicken pox and is also known to have a bitter taste.[10] E-EPO is a pH-sensitive polymer that masks the bitter taste of CPM by physically encapsulating the drug and only releasing it at pH < 5.[11] This means CPM would not be released in mouth saliva, which has a pH of approximately 7.4.[12] In particular, we study in detail the production of the loaded and unloaded fibers so as to provide a guide for others intending to use this polymer in nanofiber formulations and also to provide insights into the potential effects of drug addition on spinning parameter optimization. In addition, we investigate the taste of the fibers using a biosensor approach so as to allow early screening and product optimization to facilitate the design of the final dosage form.

Electrospinning production is influenced by a number of parameters that can be generally classified as solution, process, and environmental factors which have been widely studied for small-scale production.[13] Desired characteristics of a fiber can range from morphological to pharmaceutical activity considerations, while the range of manufacturing parameters, and the possibility of their interaction on influence, render a single parameter approach inappropriate and necessitate multifactorial methodologies in order to identify key production characteristics.

For pharmaceuticals, a systematic understanding of parameter influence is extremely helpful. Although there are several studies that have involved factorial or design of experiment (DoE) approaches,[14−23] for electrospinning there is a particular need for pharmaceuticals for information pertinent to quality by design (QbD) approaches; these allow for the quality of an end product to be built in by design, rather than reaching these attributes empirically. This is in line with the recommendations given by the ICH Q8 pharmaceutical development guidelines.[24]

The DoE in this study was used to screen for the most influential factors in producing smooth E-EPO nanofibers. Smooth fibers were defined as fibers with no bead-on-strings and those that have the most uniform fiber diameter distribution. The factors chosen to be controlled represent the critical material attributes (CMAs) and were polymer concentration and solvent mixture. The critical process parameters (CPPs) explored were flow rate, applied voltage, and gap distance. The output criteria of smooth fibers represent the critical quality attributes (CQAs) of the fibers formed. Figure 1 shows a summary of the DoE design space. Once E-EPO fibers were electrospun with and without the drug, taste-masking assessment of CPM-loaded fibers was performed.

The electronic tasting system, or E-tongue, uses potentiometric measurement principles to assess the taste of a substance as compared to a reference material.[25] Thus, the taste-masking

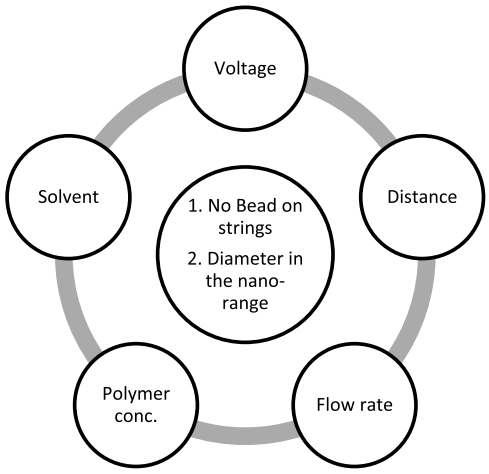

Figure 1. DoE design space, with CQAs in the inner circle and CPPs/CMAs in the peripheral circles.

efficiency of electrospun CPM fibers was assessed compared to that of placebo fibers and physical mixtures in order to establish that the optimized fibers had the potential for effective taste-masking. To our knowledge, this is the first study to use an e-tongue for taste assessment of electrospun nanofibers. In this manner, it is intended that the study may provide a blueprint for the design and characterization of taste-masked electrospun fibers, the approach being designed with a view to both pharmaceutical production requirements and therapeutic acceptability.

2. EXPERIMENTAL SECTION

2.1. Electrospinning. *2.1.1. Preparation of Precursor Solutions.* E-EPO, described as basic butylated methacrylate copolymer in the European Pharmacopoeia, is a white powder with an average molar mass of approximately 47 000 g/mol;[26] the polymer was kindly donated by Evonik (Darmstadt, Germany). E-EPO solutions were prepared by dissolving 15−50% w/v E-EPO in absolute ethanol or ethanol in combination with water. The mixture was then magnetically stirred at a temperature of 40 °C for 2−3 h. The solution was allowed to rest for a day at ambient conditions before electrospinning. Drug-loaded E-EPO solutions were prepared by adding CPM directly to the polymer solution in drug to polymer ratios of 1:2 to 1:10. CPM was purchased from Cambridge Bioscience (Cambridge, UK).

2.1.2. Manufacturing. A Spraybase electrospinning instrument (Spraybase, Dublin, Ireland) was used to manufacture the fibers. In the electrospinning process, the prepared solution was drawn in a 5 mL Terumo syringe (Surrey, UK), attached to a syringe pump. The syringe was connected to a stainless steel needle, with a diameter of 0.7 mm, via a connector tube. The viscous solution was fed through the needle at flow rates between 0.5 and 2 mL/h. Applied voltages up to 25 kV were applied to the polymer solutions, evaporating the solvent, allowing the solid fibers to deposit on a grounded metal plate collector (14.5 × 23 cm). The collector was covered in aluminum foil for ease of fiber removal. The gap distance between the needle and the collector plate was set between 150 and 200 mm. Room temperature (°C) and relative humidity (RH) (%) readings were recorded. The temperature ranged between 19 and 28 °C, and the RH ranged between 27 and 45%.

DOI: 10.1021/acs.molpharmaceut.9b00159
Mol. Pharmaceutics 2019, 16, 2557−2568

2.2. Viscosity. Viscosity measurements of E-EPO at increasing concentrations were taken to determine the chain entanglement concentration. The viscosity of samples was measured using a Bohlin Gemini HR nano dynamic rheometer at a shear stress of 1−30 Pa. Instantaneous viscosity values quoted are those recorded at a shear stress of approximately 5 Pa.

2.3. Conductivity and pH. The conductivity and pH of samples were measured using a SciQuip 902 conductivity meter. The probes were calibrated using reference solutions as per the manufacturer's instructions.

2.4. Experimental Design. A DoE approach was utilized to optimize the electrospinning of E-EPO on its own using a definitive screening design. Definitive screening designs help to detect the main effects of input parameters on a particular outcome in the most efficient way possible.[27] JMP Pro 12.0.1 (SAS Institute) was used for experimental design, predictive modeling, and data analysis. Smooth nonbeaded fibers, with a reduced fiber diameter, were set as the desired output criteria. Five factors were investigated at three levels of each, as shown in Table 1. The experiments were performed over two different days or blocks. The sequence in which these runs were carried out was randomized to reduce variability. The data were fitted to a standard least squares model, yielding linear regression and analysis of variance (ANOVA) results.

Table 1. Factors Investigated in the Electrospinning of E-EPO Using a Definitive Screening Design

factor	low	medium	high
applied voltage (kV)	10.00	17.50	25.00
flow rate (mL/h)	0.50	1.25	2.00
gap distance (mm)	150	200	250
E-EPO concentration (% w/v)	25.00	35.00	45.00
water in solvent (% v/v)	0.00	10.00	20.00

2.5. Scanning Electron Microscopy (SEM). A sample of the fiber collected was adhered onto aluminum scanning electron microscopy (SEM) stubs (TAAB Laboratories, UK) using a carbon-coated double-sided tape. To render them conductive, a thin coating of gold was applied in a Quorum Q150T sputter coater (Quorum Technologies Ltd. East Sussex, UK) in an argon atmosphere. A scanning electron microscope FEI Quanta 200 FEG (FEI, USA) was used to image the fiber morphology. ImageJ 1.46R software (NIH, Maryland, USA) was used to measure the diameters of the fibers imaged. OriginPro 9.4 (Origin Lab, Massachusetts, USA) was used to construct the histograms of fiber diameter distributions.

2.6. Thermogravimetric Analysis (TGA). Thermogravimetric analysis (TGA) of pure drug, polymer, physical mixtures, placebo fiber, and drug-loaded fibers was carried out using a TA Instruments Hi-Res 2950 thermogravimetric analyzer (TA Instruments, New Castle, Delaware, USA). A purge nitrogen gas flow rate of 60 mL/min was used for the furnace and 40 mL/min for the TGA head. Samples (mass 5−15 mg) were analyzed in open aluminum PerkinElmer pans with a heating rate of 10 °C/min from 30 to 500 °C. Data analysis was carried out with TA Universal Analysis software, version 4.5A.

2.7. Differential Scanning Calorimetry (DSC). Modulated temperature differential scanning calorimetry (MTDSC) thermograms of pure drug, polymer, physical mixture, and electrospun fibers were recorded using a TA Instruments Q2000 calorimeter (TA Instruments, New Castle, Delaware, USA). Sample weights ranged from 4 to 8 mg and were sealed in a 40 μL aluminum PerkinElmer standard pan. A pinhole was manually formed in the lids to allow for solvent evaporation. Samples were heated under nitrogen gas (flow rate 50 mL/min) at a heating rate of 2 °C/min ramped up to 150 °C, amplitude ±0.212 °C, and a period of 40 s. Data analysis was carried out with TA Universal Analysis software, version 4.5A.

2.8. Powder X-ray Diffraction (XRD). Solid state characterization of CPM and E-EPO before and after electrospinning was completed using a Rigaku MiniFlex 600 X-ray diffractometer (Rigaku, Tokyo, Japan). Cu Kα radiation was operated at 40 mV and 15 mA. Patterns were recorded over the 2θ range 3°−40° at a scan rate of 3 or 5°/min, with an interval of 0.02° or 0.005°, respectively. RAW files produced were converted to X-ray diffraction (XRD) data files using PowDLL version 2.51 file converter software. The data were then viewed on X'Pert Data Viewer version 1.2F.

2.9. Fourier Transform Infrared Spectroscopy (FTIR). Fourier transform infrared spectroscopy (FTIR) studies were performed using a Spectrum 100 FTIR spectrometer (PerkinElmer, USA), and spectra were collected in the range of 4000−650 cm^{-1} with a total of 16 scans and a resolution of 2 cm^{-1}, unless otherwise stated. Background scans were performed in all experiments.

2.10. Determination of Drug Loading. λ_{max} of CPM was determined by scanning CPM at a concentration range of 5−50 μg/mL between 200 and 300 nm, with steps of 5 nm, using a UV−vis spectrophotometer, SpectraMax (San Jose, CA, USA). Data were collected using SoftMax Pro software. Standard solutions of CPM with the concentration range of 5−50 μg/mL were prepared in ethanol. A standard curve (R^2 = 0.9988) of CPM was plotted using absorbance data recorded using a Jenway 6305 UV−vis spectrophotometer (Bibby Scientific, Staffordshire, UK). Absorbance was recorded at 205 nm (λ_{max}). Drug loading was calculated by using the slope = 0.07525 and intercept = 0.03447 of the standard curve.

2.11. Statistical Analysis. All experiments were conducted in triplicate unless otherwise stated. All data were presented as mean value ± standard deviation. Statistical significance was taken at p-value < 0.05.

2.12. E-Tongue Taste Assessment. *2.12.1. Measurement Procedure.* The TS-5000Z (Insent Inc., Atsugi-shi, Japan) was equipped with four lipid membrane sensors and two corresponding reference electrodes (New Food Innovation Ltd., UK). Positively charged membrane sensors included C00, responding to acidic bitterness, and AE1, responding to astringency. Negatively charged membrane sensors included AC0 and AN0, both responding to basic bitterness at different sensitivity and selectivity levels.

The reference solution was prepared by dissolving 30 mmol/L potassium chloride and 0.3 mmol/L tartaric acid in distilled water. The negatively charged membrane washing solution was prepared by diluting absolute ethanol to 30% v/v with distilled water, followed by the addition of 100 mmol/L hydrochloric acid. The positively charged membrane washing solution was prepared by diluting absolute ethanol to 30% v/v and adding 100 mmol/L potassium chloride and 10 mmol/L potassium hydroxide to the mixture. Tartaric acid, potassium chloride, and potassium hydroxide were obtained from Sigma-Aldrich (UK). Iso-alpha acid was obtained from Insent (Atsugi-shi, Japan). Hydrochloric acid was obtained from Fisher Chemicals (Loughborough, UK). All substances were used as received. A sensor check was conducted routinely before each measurement

DOI: 10.1021/acs.molpharmaceut.9b00159
Mol. Pharmaceutics 2019, 16, 2557−2568

to ensure that the sensors were working within the correct millivolt range.

Each measurement cycle consisted of measuring reference potential (V_r) in reference solution, followed by the measurement of electric potential (V_s) of the sample solution; $V_s - V_r$ represented the initial taste.[28]

The sensors were finally refreshed in alcohol solutions before measurement of the next sample.

2.12.2. Sample Preparation. Taste extracted liquids were used for biosensor assessment. The dose unit of CPM was set at 1 mg. For taste evaluation, 20 dose units (equivalent to 20 mg of CPM) were added to 100 mL of 10 mmol potassium chloride solution, as a supporting electrolyte, at 37 °C and gently stirred for 1 min. This represented a concentration of one dose in 5 mL, which was suitable for taste assessment as there was only slight dilution of the sample. The mixture was then filtered through 0.22 μm filters (Merck-Millipore, Cork, Ireland), removing any suspended particles.

2.12.3. Data Analysis. All measurements were repeated four times. The data from the first run were discarded to allow for the conditioning of sensors. In this study, a solution of 10 mmol potassium chloride was used as a control sample, and the corresponding sensor responses were subtracted from the sensor responses of the samples. Hence, all data produced are a mean of three measurements and represent relative sensor responses. Multivariate principal component analysis (PCA) was performed on the data collected. This aided visualization of the high number of data points on a two-dimensional map. Differences between samples were assessed by determining the Euclidean distances, which were calculated from the cluster center.[29] All data analysis was carried out using OriginPro 9.4 (Origin Lab, Massachusetts, USA).

3. RESULTS AND DISCUSSION

3.1. Chain Entanglement Concentration. Concentrations of E-EPO ranging from 20 to 50% w/v were electrospun and the solution viscosity was characterized to determine a chain entanglement concentration as described by Kong and Ziegler.[30] This is defined as the intercept between the two fitted lines representing untangled and entangled regions, as shown in Figure 2. The chain entanglement concentration represents the point at which smooth fibers start to form and is therefore significant for the viability of electrospinning;[31,32] this was found to be at 32.5% w/v for E-EPO.

To support the viscosity measurements, SEM visual representation of the electrospun E-EPO fibers is shown in Figure 3.

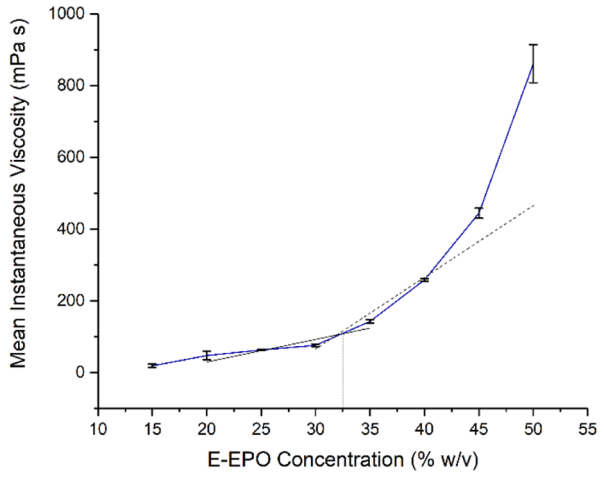

Figure 2. Instantaneous viscosity at a shear stress of 5 Pa as a function of E-EPO concentration.

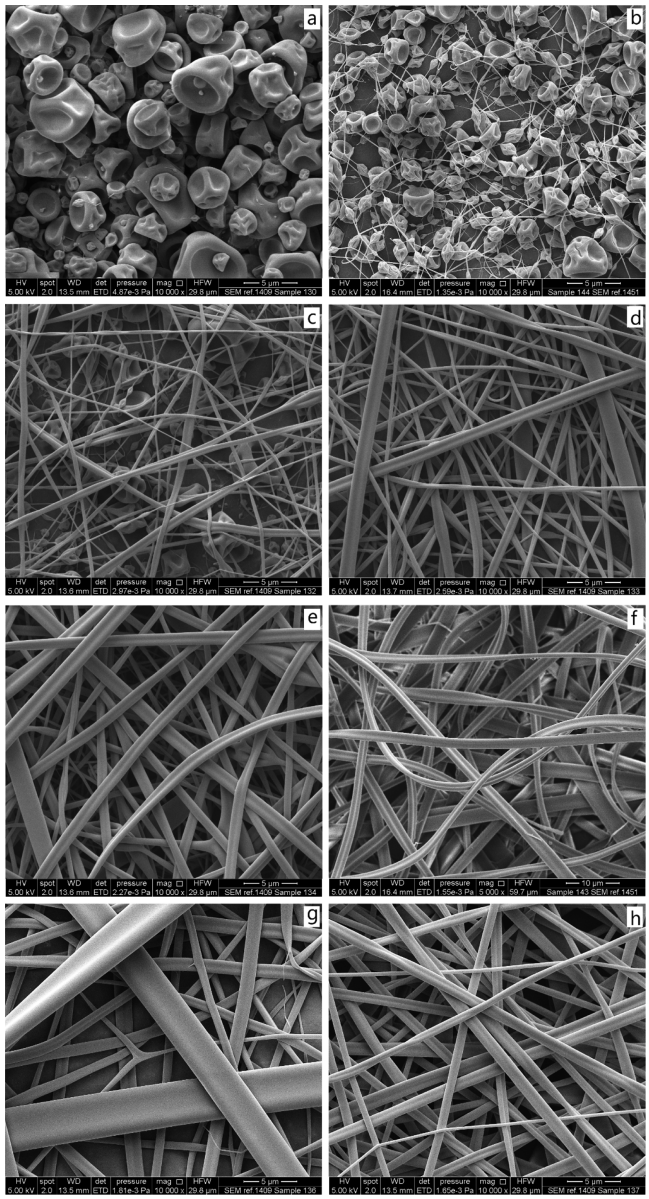

Figure 3. SEM images of electrospun E-EPO fibers: (a) 15, (b) 20, (c) 25, (d) 30, (e) 35, (f) 40, (g) 45, and (h) 50% w/v. All fibers were processed at applied voltages of 10−20 kV, a flow rate of 1 mL/h, a gap distance of 200 mm, a temperature of 26 °C, and a RH of 32%.

Figure 3a−c shows the occurrence of electrospraying at 15 and 20% E-EPO. As the polymer concentration increases, a transition between spraying and electrospinning occurs. Fiber formation starts at 25% E-EPO; however, it was not until 30% E-EPO that smooth fibers were formed (Figure 3d). Figure 3e−h also shows smooth fibers with no bead-on-strings. Although fibers are smooth at this stage, it can be seen from Figure 4 that as the polymer concentration increases, the fiber diameter also increases, which can be attributed to the fact that more polymer was dispensed through the needle. It can be observed that the

DOI: 10.1021/acs.molpharmaceut.9b00159
Mol. Pharmaceutics 2019, 16, 2557−2568

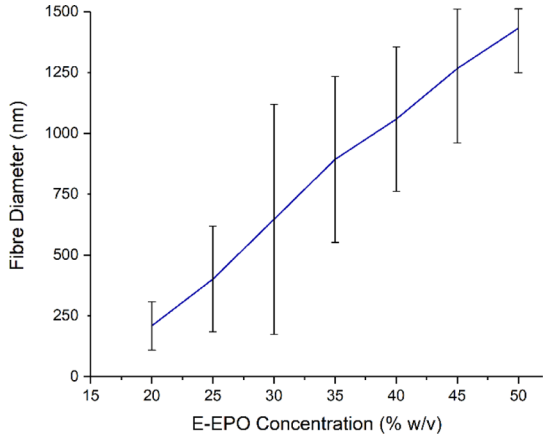

Figure 4. Mean fiber diameter vs concentration of E-EPO. The error bars represent the fiber diameter distribution at each concentration.

fibers formed are ribbonlike, and this was likely to be due to the rapid evaporation of the solvent causing the fiber to collapse and appear flat.[33]

3.2. DoE Definitive Screening Design. The DoE definitive screening design aimed to screen the most influential factors affecting fiber diameter and beading, thus facilitating the optimization of the electrospinning process. This type of DoE requires only a small number of runs to identify most important factors quickly and efficiently. Table 2 shows the parameters investigated, the levels tested for each, and the associated results.

If a systematic approach was used to run experiments for all combinations of the five chosen factors at three levels for each, this would have resulted in 3^5 or 243 separate experiments. The design allowed for screening with only 14 runs, investigating the main effects of the parameters on the outputs: diameter and beading.

From Table 2, it can be seen that samples 7 and 12 were both run at the same conditions, known as center points (CP) of the design. It was noted that sample 12 yielded beaded fibers, while sample 7 was electrospun into smooth fibers. It is well documented that environmental conditions affect electrospun fibers, and it is a factor that needs to be taken into consideration with electrospinning.[34]

Figure 5 shows the statistical significance level of each of the parameters investigated on both outputs when modeled

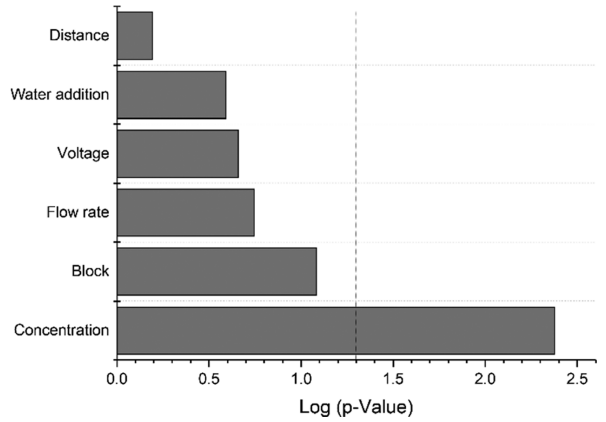

Figure 5. Pareto chart showing the statistical significance of the various parameters in producing bead-free fibers with a small diameter. The vertical dashed line represents the significance level of log *p*-value = 0.05.

together. *P*-value is expressed on the log scale; the vertical dashed line represents the statistically significant level of log(*p*-value) = 0.05. Polymer concentration was found to be the only statistically significant factor. If increased, it reduced beading defects, whereas if decreased, it reduced the fiber diameter.

3.2.1. Fiber Diameter. The effect of adding water to ethanol in the solvent mixture was not found to be a statistically significant factor for E-EPO fiber diameter reduction (*p*-value = 0.2572). Water increases the dielectric constant of the solvent and can lead to a reduced diameter of the fiber because of increased stretching of the fibers, as in the case of sample 11, where the addition of 20% v/v water to the solvent yielded a mean fiber diameter of 2789 ± 677 nm. On the other hand, sample 4 had no water in the solvent mixture, and it had a mean fiber diameter of 4207 ± 78 nm. Water addition can also increase the viscosity of a solution and therefore can lead to an increased diameter, as is the case with sample 2 (20% v/v water), yielding a diameter of 3078 ± 741 nm, as compared to sample 1 (10% v/v water), which yielded a diameter of 2358 ± 782 nm.[35]

Table 2. DoE Definitive Screening Design: Parameters Investigated and Findings

sample	block	applied voltage (kV)	flow rate (mL/h)	gap distance (mm)	water (% v/v)	E-EPO conc. (% w/v)	beading[a]	pH	conductivity (μS/cm)	viscosity (mPa s)	diameter (nm)
1	1	25	2	150	10	45	0	8.4	6.20 ± 0.4	1650 ± 43	2358 ± 782
2	1	17.5	2	250	20	45	0	8.9	5.65 ± 0.6	2068 ± 47	3078 ± 741
3	1	25	1.25	150	20	25	105	8.7	9.57 ± 0.5	76 ± 6	259 ± 58
4	1	10	1.25	250	0	45	0	8.3	2.03 ± 0.2	444 ± 14	4207 ± 78
5	1	10	0.5	250	10	25	NF	8.6	6.38 ± 0.3	51 ± 6	N/A
6	1	17.5	0.5	150	0	25	60	8.7	3.24 ± 0.4	63 ± 2	483 ± 181
7	CP-1	17.5	1.25	200	10	35	0	8.9	5.01 ± 0.2	176 ± 17	1574 ± 535
8	2	25	2	250	0	25	145	8.9	3.24 ± 0.4	63 ± 2	416 ± 359
9	2	25	0.5	200	0	45	0	8.9	2.03 ± 0.2	444 ± 14	2557 ± 395
10	2	10	2	200	20	25	NF	9.2	9.57 ± 0.5	76 ± 6	N/A
11	2	10	0.5	150	20	45	0	9.2	5.65 ± 0.6	2068 ± 47	2789 ± 677
12	CP-2	17.5	1.25	200	10	35	65	8.7	5.01 ± 0.2	176 ± 17	436 ± 162
13	2	25	0.5	250	20	35	65	8.9	6.90 ± 0.2	133 ± 25	260 ± 68
14	2	10	2	150	0	35	NF	8.5	2.17 ± 0.1	143 ± 5	N/A

[a]Approximate number, counted in SEM ×5000 mag image. NF recorded when spraying occurred and no fibers were formed—those data were excluded from prediction.

DOI: 10.1021/acs.molpharmaceut.9b00159
Mol. Pharmaceutics 2019, 16, 2557−2568

Similar to the addition of water, the applied voltage was not found to be statistically significant in reducing the diameter of E-EPO fibers (p-value = 0.2197). Nonetheless, as the applied voltage increases, the electric field is enhanced accelerating the jet, and hence, its stretching gives rise to smaller fibers. However, although minor, an increase in applied voltage can also cause an increase in polymer drawn, thereby increasing the fiber diameter. Therefore, depending on conditions, it can lead to either an increase or a decrease or it has no effect at all on fiber diameter. Although an increase in flow rate was observed to show an increase in fiber diameter, this was not found to be statistically significant (p-value = 0.8203). An increase in gap distance increases the flight jet time and elongates the polymer jet stretching out and therefore can reduce the fiber diameter, but it was also not found to be statistically significant (p-value = 0.6413).

The screening design showed that out of those parameters studied in the stated ranges, polymer concentration was the only statistically significant factor in reducing the fiber diameter (p-value = 0.0076).

The ANOVA data show that the input parameters studied explain the reduction in mean fiber diameter observed. The error's sum of squares is less than the model's sum of squares, and therefore, the variance in the fiber diameter is explained by the statistically significant effect of the input parameters (p-value = 0.0362) and not by pure chance or error. The sum of errors is shown as the corrected total or C. total. The degrees of freedom (DF) represent how many values in the calculation have the freedom to vary, and they are equal to the number of observations minus the number of parameters studied in the model. The model's DF is 6 because out of 14 runs, 2 observations were eliminated as no electrospinning occurred; 12 minus 6 parameters (applied voltage, flow rate, gap distance, solvent, polymer concentration, and block) equates to 6 DF. The ANOVA data are shown in Table 3.

Table 3. ANOVA Data for Reduced Diameter

source	DF	sum of squares	mean square	F ratio
model	6	17 828 619	2 971 437	7.4530
error	4	1 594 765	398 691	prob > F
C. total	10	19 423 384		0.0362

3.2.2. Beading. The effect of water addition was not found to be statistically significant on beading (p-value = 0.2572). The addition of water increased the conductivity of the solutions, which reduced beading on some occasions; however, in other instances, beading increased because water was not evaporating by the time the fibers deposited on the collector. An increase in applied voltage can reduce beading by improving Taylor cone stability through overcoming the surface tension and eventually stopping dripping.[36] This effect was not statistically significant on the reduction of beading in E-EPO fibers (p-value = 0.7778). Flow rate can increase beading as it can lead to Taylor cone instability and therefore interruption of the jet stream. This however was not found to be statistically significant on reducing beading (p-value = 0.8203). An increase in gap distance can lead to increased beading because of a weakened electric field and therefore reduced solvent evaporation.[37] However, this effect was not found to be statistically significant on the reduction of beading (p-value = 0.6966). Similar to its effect on fiber diameter, polymer concentration was the only statistically significant parameter in reducing beading (p-value = 0.0042).

Figure 6 shows SEM images of sample 7 and sample 11 fibers. At 35% w/v E-EPO, smooth fibers are formed. At 45% w/v E-EPO, smooth fibers are also generated; however, needle clogging becomes very problematic at this high concentration. Cleaning of the needle tip manually was repeated, which would have resulted in discontinuation of a single continuous fiber. This has therefore been identified as a rate-limiting factor, and E-EPO was not recommended to be electrospun at concentrations any higher than 35% w/v.

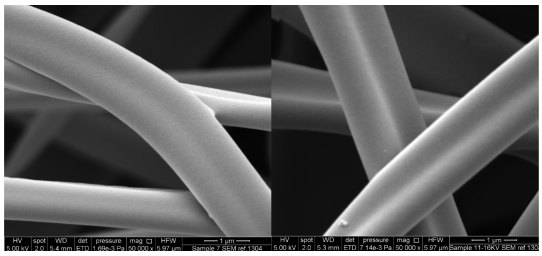

Figure 6. Left: DoE sample 7, 35% w/v E-EPO, 10% v/v water in solvent; process parameters: 17.5 kV, 1.25 mL/h, and 200 mm. Right: DoE sample 11, 45% w/v E-EPO, 20% v/v water added in solvent; process parameters: an applied voltage of 10 kV, a flow rate of 0.5 mL/h, and a gap distance of 150 mm.

The ANOVA data show that the input parameters studied explain the reduction in beading observed. The error's sum of squares is less than the model's sum of squares, and therefore, the variance in the beading recorded is explained by the statistically significant effect of the input parameters (p-value = 0.0287) and not by pure chance or error. The ANOVA data are shown in Table 4.

Table 4. ANOVA Data for Reduced Beading

source	DF	sum of squares	mean square	F ratio
model	6	24573	4095	8.5
error	4	1926	481	prob > F
C. total	10	26 500		0.0287

3.3. Optimization. Using standard least squares regression analysis model, a predictive tool was used to predict fiber diameter and beading number. To determine the reliability of the predictive model, a summary of the fit is shown in Figure 7. The regression model for the reduction of fiber diameter data had an R^2 of 0.92, which means that 92% of the predicted diameters are within the confidence intervals of the actual diameters recorded. Similarly, the predicted beading regression analysis, R^2 = 0.93, also had a very positive correlation with the actual beading numbers recorded, showing that 93% of the model predictions are within the confidence intervals of the actual beading data recorded. Both confidence curves cross the horizontal lines, which indicate that the predictions are statistically significant to the actual measurements.

3.3.1. Minimizing Beading. As well as screening key parameters, the definitive screening design was used to predict optimum conditions. For bead-free fibers, these were predicted to be 45% w/v E-EPO, 20% v/v water, flow rate of 0.9 mL/h, applied voltage of ~21 kV, and gap distance of 150 mm, with an R^2 of 0.93, as shown in Figure 7. This was validated experimentally, thereby lending weight to the predictive approach (temperature: 19 °C, RH 32%) The fibers had a mean diameter of 4317 ± 1942 nm.

DOI: 10.1021/acs.molpharmaceut.9b00159
Mol. Pharmaceutics 2019, 16, 2557−2568

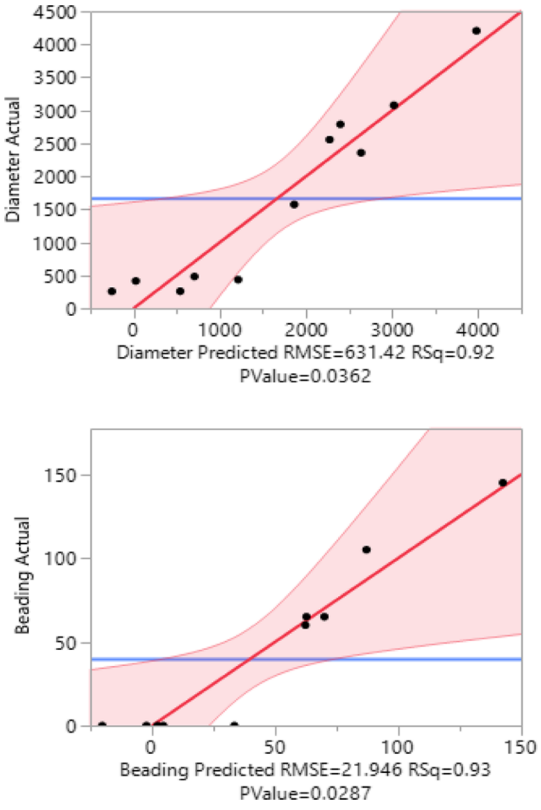

Figure 7. Summary of fit predicting the diameter and number of beads in electrospun E-EPO fibers. Block line represents the linear fit and dashed outer lines represent the confidence curve, while the horizontal dashed line represents the hypothesized predicted outcomes at optimum conditions.

3.3.2. Minimizing Diameter. Minimizing fiber diameter was most affected by a decrease in polymer concentration (p-value = 0.008). The optimum parameters were predicted to be 28% w/v E-EPO and 20% v/v water at a flow rate of 0.5 mL/h, an applied voltage of 25 kV, and a gap distance of 150 mm to generate fibers with a mean diameter of 155 nm, R^2 = 0.92. Experimental validation produced nonbeaded fibers with a mean diameter of 930 nm (±348), temperature 28 °C, and RH 36%.

3.3.3. Minimizing Beading and Diameter Together. When both outcomes were modeled together, the prediction profiler tool, shown in Figure 8, predicted that at 25 kV, 35% w/v E-EPO, 0.5 mL/h flow rate, a gap distance of 150 mm, and an addition of 20% v/v water, fibers with a mean diameter of 621 nm will be formed. They will also contain 37 beads per 3 mm^2 (i.e., very low beading). When validated experimentally, nonbeaded fibers with an average diameter of 1904 nm (±705) were formed; temperature: 28 °C, RH 36%.

An SEM image shows the fibers produced and a histogram of fiber diameter distribution in Figure 9.

3.4. Addition of CPM. CPM was initially electrospun with E-EPO at ratios ranging from 1:2 to 1:6, CPM/E-EPO; it was shown that fiber formation started to occur at ratios above 1:4. Electrospinning does not occur below this drug load, and this is likely due to the fact that the highly charged CPM molecules repel and cause the jet to split into particles rather than to deposit as the fibrous material. CPM was then added using the defined optimized electrospinning condition ranges of E-EPO at drug ratios of 1:6, 1:7, 1:8, 1:9, and 1:10. Input and output parameters, namely, pH, fiber diameter, and drug-loading measurements were recorded. The pH of E-EPO and CPM solutions had a mean value of 7.49 ± 0.2. This is neutral and therefore should not be irritating for the oral mucosa, which is an important consideration because the fibers are formulated for oral drug delivery. Electrospinning was completed at temperatures of 21.8 ± 2.03 °C and RH of 34.5 ± 11%.

The drug loadings in Table 5 show good agreement with theoretical entrapments; it is intended that the drug-loaded fiber mats would eventually be administered to children in an age-appropriate formulation such as a mini tablet or oral film. If the 1:0 formulation were to be used, using the actual drug-loading values, it can be seen than approximately 10 mg of fiber would need to be ingested to deliver the clinical dose of 1 mg. CPM's dosage ranges from 1 mg twice a day for young infants to 1−4 mg up to 4 times a day in older children.[38]

As expected, in the presence of CPM, the average E-EPO fiber diameter increases steadily as the polymer concentration was increased.

The SEM images of drug-loaded fibers at 1:6, 1:8, and 1:10 CPM/E-EPO are shown in Figure 10. It can be seen that as the

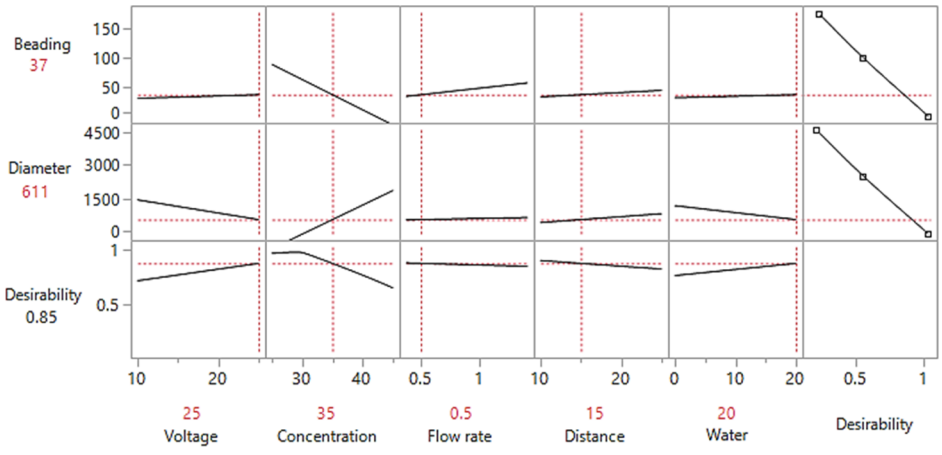

Figure 8. Prediction tool showing the relationship between the input parameters and outcome. The x-axis represents input parameters and the y-axis represents the outcomes predicted and the desirability. The desirability column shows negative sloped lines, indicating the desire to minimize beading and fiber diameter. The dashed lines show the intersection between the values of the input and output parameters. The block lines show the relationship between input parameters and the outputs.

DOI: 10.1021/acs.molpharmaceut.9b00159
Mol. Pharmaceutics 2019, 16, 2557−2568

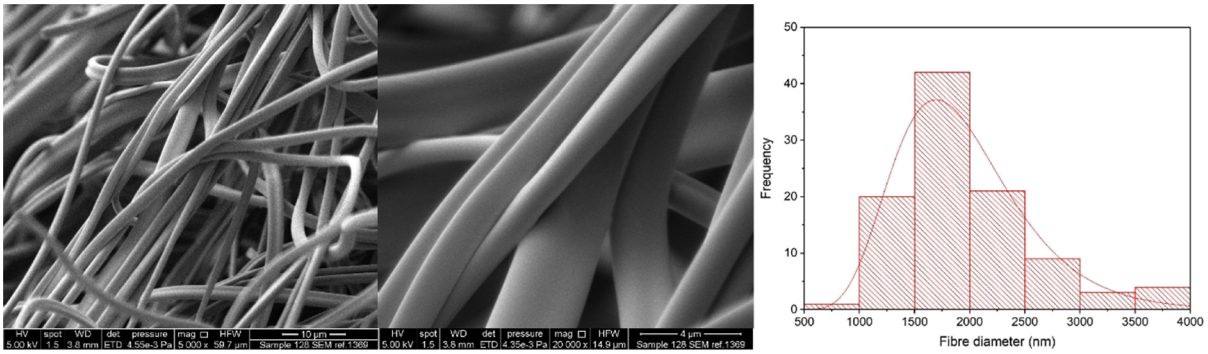

Figure 9. SEM image of electrospun 35% w/v E-EPO, DoE predicted parameters for bead-free fibers in the nanorange: an applied voltage of 25 kV, a flow rate of 0.5 mL/h, and a gap distance of 150 mm. A histogram showing fiber diameter distribution of $n = 100$.

Table 5. Drug-Loading Values of Electrospun Fibers

CPM/E-EPO	theoretical drug load (%)	actual drug load (%)
1:6	14.3	15.4 ± 2.6
1:8	11.1	9.8 ± 0.3
1:10	9.1	9.3 ± 0.6

drug loading was reduced, smoother fibers were formed, with a smaller average diameter. The drug load therefore was significant on the viability of electrospinning. The poor formation of fibers at a high drug load was due to the increased conductivity of the solution, which causes repulsion in the jet stream and thereby impedes the formation of smooth fibers.

It can be seen from the fiber diameter histograms that as the drug amount added was decreased, the fiber diameter decreases

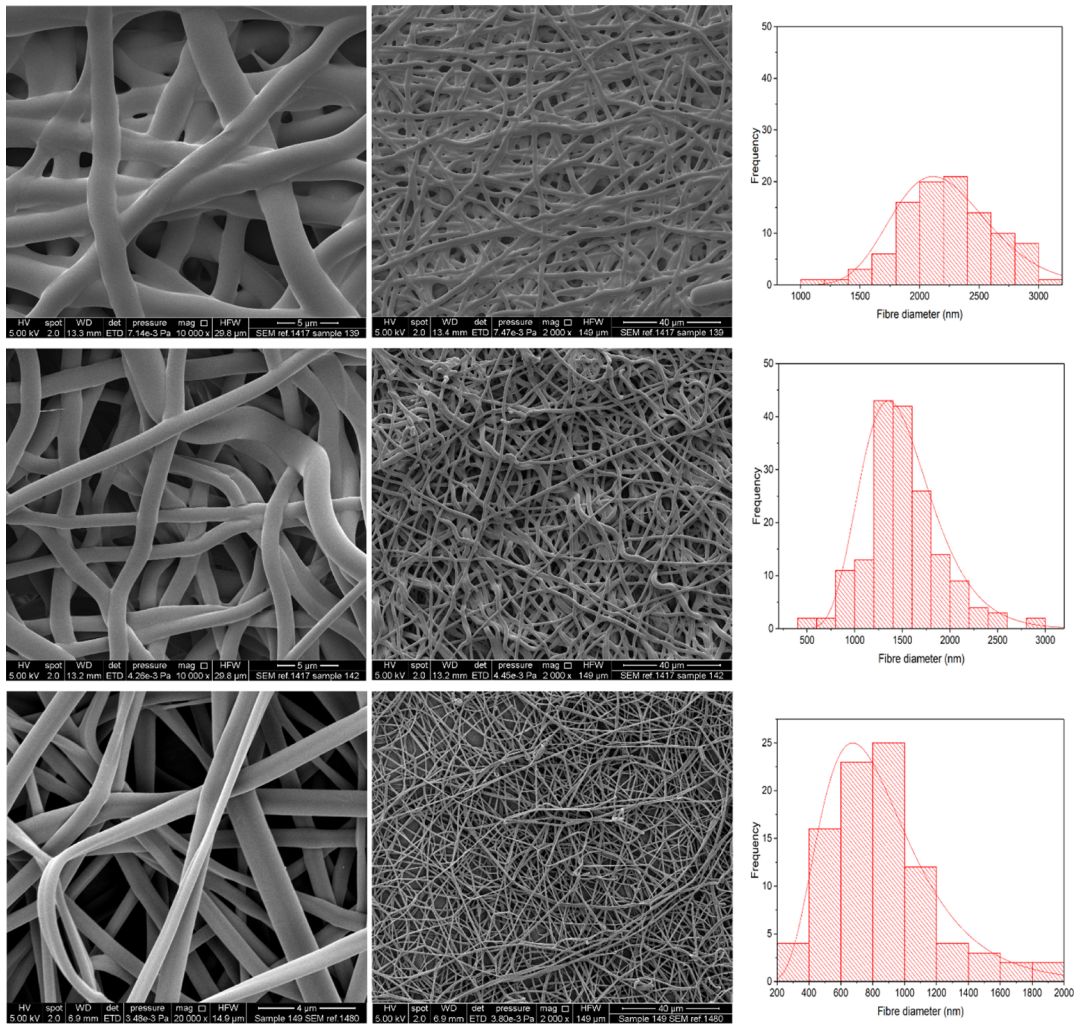

Figure 10. SEM images and histograms showing diameter distribution of 35% w/v E-EPO electrospun fibers at an applied voltage of 15 kV, a flow rate of 1 mL/h, and a gap distance of 175 mm. Top—1:6 CPM/E-EPO. Middle—1:8 CPM/E-EPO. Bottom—1:10 CPM/E-EPO.

DOI: 10.1021/acs.molpharmaceut.9b00159
Mol. Pharmaceutics 2019, 16, 2557−2568

steadily. Smoother fibers were also formed as the drug loading reduced; this was probably due to the fact that there are less charged species, and therefore, repulsive forces are reduced, allowing for better fiber formation. As the drug loading was increased, the conductivity increases, and in the presence of water, this is even higher. Because drug-loaded solutions are being highly conductive, multiple jets form at the nozzle, and this may explain the large range of fiber diameter distribution seen.

3.5. Multifactorial Interactions. The main effects of polymer concentration, water addition, applied voltage, flow rate, gap distance, and the addition of a drug have so far been discussed in the electrospinning of E-EPO. The DoE completed for manufacturing optimization of E-EPO aimed at screening for the most influential factors. Multifactorial interactions are useful to gain a deeper understanding of the electrospinning process. Forty-two experiments of drug-loaded E-EPO were completed. The effect of each parameter and multifactorial interactions were investigated on reducing the fiber diameter. Beading was not explored at this stage, as it was completely eliminated by electrospinning the drug-loaded solutions above the critical entanglement concentration of E-EPO.

Figure 11 shows that both polymer concentration and flow rate had statistically significant effects on reducing the fiber

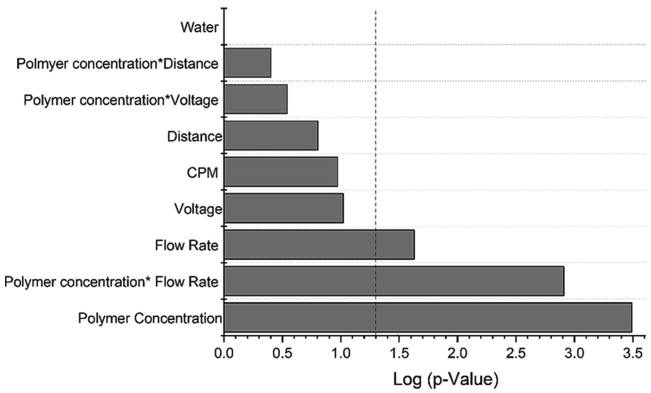

Figure 11. Pareto chart showing the statistical significance of the various parameters in producing drug-loaded E-EPO fibers with a small diameter. The vertical dashed line represents the significance level of log *p*-value = 0.05.

diameter of drug-loaded E-EPO fibers. It is to be noted that the flow rate's significant effect was likely not due to the drug addition in itself versus E-EPO on its own but due to the higher number of experiments run and therefore increased power.

The interaction between the flow rate and polymer concentration also played a role in affecting the fiber diameter and was found to be statistically significant. The variation of one of those parameters can influence the effect of the other on the outcome. At a low polymer concentration, the fiber diameter is decreased; however, a sufficient flow rate is needed to ensure the feasibility of the electrospinning process and the formation of a continuous Taylor cone and therefore the production of fibers. This interaction is in line with the findings of Ruiter et al.[21]

3.6. Thermogravimetric Analysis. The degradation profiles for pure E-EPO and CPM were analyzed using TGA. Minimal solvent loss (<1% of weight) was observed in the temperature range for water evaporation. Data observed from the TGA measurements were used to determine temperature ranges for DSC measurement. Similar to the raw materials, minimal solvent loss (<1% of weight) was observed for both the placebo and active fibers around ethanol's, 78 °C, or water's boiling point, 100 °C.[39]

3.7. X-ray Diffraction. XRD patterns in Figure 12a show distinct peaks of CPM, indicating a crystalline state, whereas E-

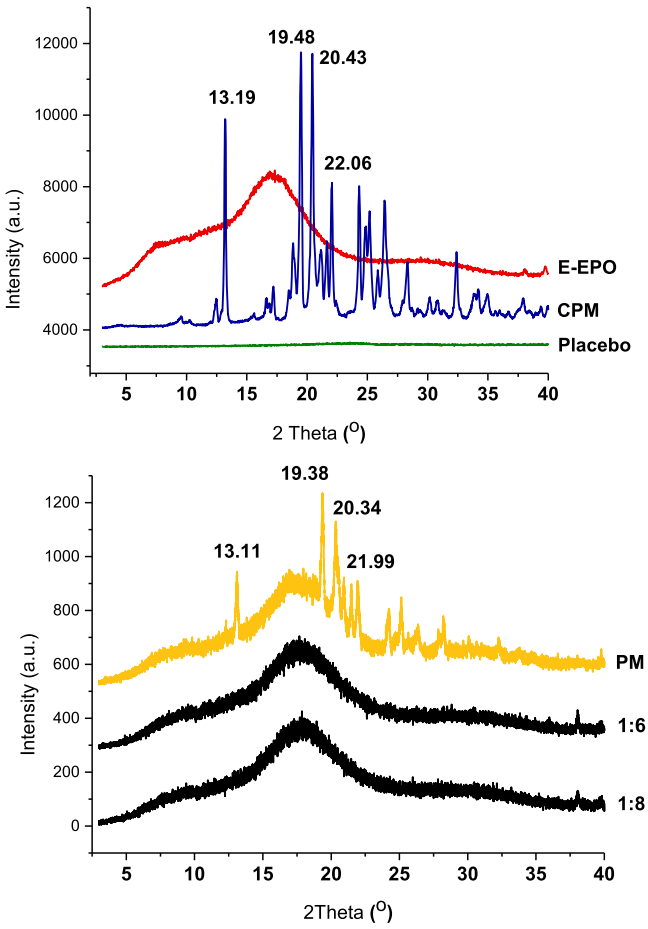

Figure 12. (a) XRD pattern of pure E-EPO, pure CPM, and placebo 35% w/v E-EPO fiber. (b) XRD pattern of E-EPO and CPM physical mixture, 35% w/v E-EPO + 1:6 CPM/E-EPO fibers and 35% w/v E-EPO + 1:8 CPM/E-EPO fibers.

EPO shows a halo that indicates an amorphous state. The placebo fiber's diffraction pattern shows a halo indicative of the amorphous state; however, it appears very flat. This is probably due to the low sensitivity slow scanning rate used at 3°/min with a step size of 0.02°. To confirm that this was the cause, drug-loaded fibers and the raw ingredients' physical mixture were recorded over the ranges of 3°−40° at a scan rate of 5°/min with a step size of 0.005°, improving the sensitivity of the diffraction pattern recorded. The diffraction pattern shown in Figure 12b shows more distinct shapes at the same intensity as that of CPM and E-EPO's physical mixture. It can be seen that the drug-loaded diffraction patterns appear as halos similar to the placebo fiber and unformulated E-EPO indicative of amorphous solid dispersion formation. This shows that CPM changes to the amorphous state following electrospinning. The rapid evaporation of solutions through electrospinning, followed by quick solid dispersion, explains the formation of amorphous single phase systems.

3.8. Fourier Transform Infrared Spectroscopy. In Figure 13, the peak observed in E-EPO at 1210 cm^{-1} is characteristic of

DOI: 10.1021/acs.molpharmaceut.9b00159
Mol. Pharmaceutics 2019, 16, 2557−2568

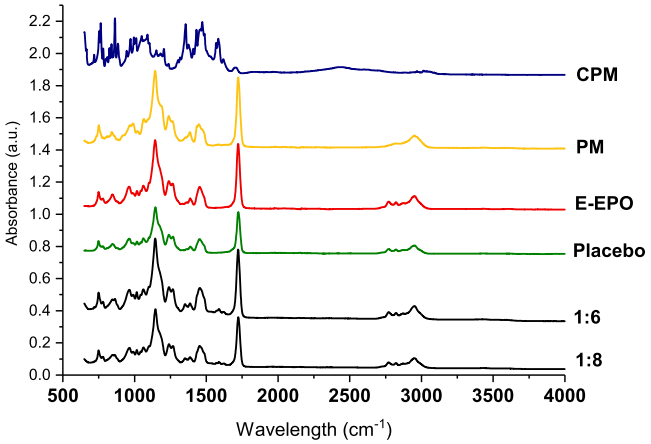

Figure 13. FTIR spectra of unformulated pure CPM, E-EPO, their physical mixture, 35% w/v E-EPO placebo fiber, and 1:6 and 1:8 CPM/E-EPO drug-loaded fibers.

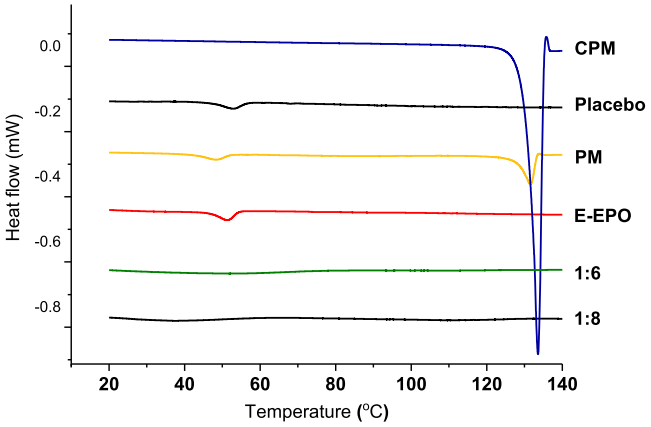

Figure 14. DSC thermogram of pure CPM, physical mixture, pure E-EPO, 35% E-EPO placebo fiber, 35% w/v E-EPO + 1:6 CPM fibers, and 35% w/v E-EPO + 1:8 CPM/E-EPO fibers. Exo up.

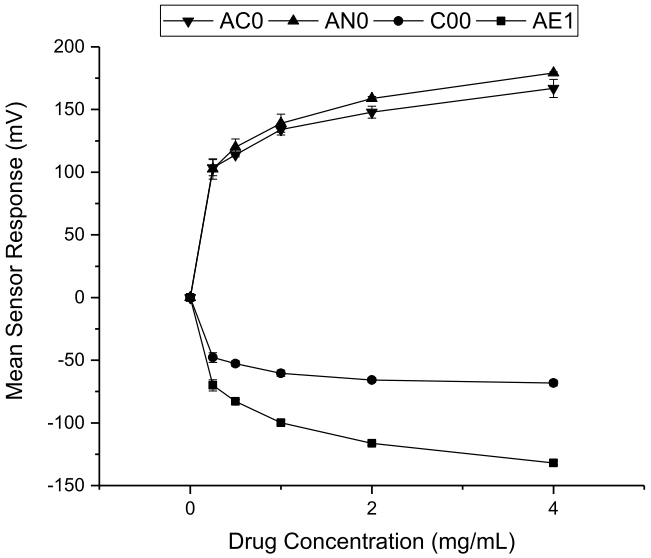

Figure 15. Analysis of sensor responses to various concentrations of CPM: AC0—basic bitterness; AN0—basic bitterness; C00—acidic bitterness; AE1—astringency.

the C−O bond and that at 1720 cm^{-1} is characteristic of the C═O bond and is present in the physical mixture and the electrospun fibers. Both the placebo fiber and the drug-loaded fiber's spectra are almost identical, indicating that no bonds were formed between the polymer E-EPO and the drug CPM, further validating the XRD data that an amorphous solid dispersion was formed.

3.9. Differential Scanning Calorimetry. MTDSC measurements were carried out to determine the melting point (T_m) of CPM and the glass transition (T_g) of E-EPO. Midpoint values were recorded. E-EPO's T_g was recorded as 50.9 °C, consistent with literature findings.[40] CPM's T_m was recorded as 133.24 °C, in close agreement with the reported literature value of 130−135 °C.[41]

When the physical mixture of CPM and E-EPO was tested, both an endothermic melting trough at 133.51 ± 0.43 °C and a T_g shift at 49.7 ± 0.89 °C were observed, indicating that both compounds were detected. The intensity of the melting peak was less in the physical mixture than in pure CPM, which could be explained by the dilution effect of the polymer.[42]

Electrospun fibers were then tested. An E-EPO placebo fiber was tested, and an endothermic shift was observed at 50.74 ± 0.66 °C, indicating a T_g shift. Drug-loaded fibers did not display a melting peak which indicates the conversion of crystalline CPM to the amorphous state. Representative DSC results are shown in Figure 14.

3.10. E-Tongue. One of the main limitations of the E-tongue is that it can only detect drugs ionizable in the medium used for the measurement.[25] The first step was to therefore determine if the drug in question, CPM, was detectable by the E-tongue's taste sensors. It was confirmed that the E-tongue can detect CPM as a bitter drug. All sensors used showed a concentration-dependent response to CPM as shown in Figure 15.

Taste sensor output was obtained by measuring a difference in electric potential between the taste sensor and the reference electrode. Table 6 shows the data for Euclidean distances between pure CPM and pure E-EPO, physical mixtures, placebo fiber, and 1:8 and 1:6 drug-loaded fibers. As anticipated, pure E-EPO and placebo fibers tested had the largest Euclidean distance, an arbitrary distance from the pure bitter drug; the higher the distance, the lower the bitterness of the sample.[43] This was followed by the drug-loaded fibers and finally by the physical mixture. Drug-loaded fibers had a larger distance than the physical mixture, indicating better taste-masking.

Table 6. Euclidean Distances for Pure E-EPO, Physical Mixture, Placebo Fiber, and Drug-Loaded Fibers from Pure CPM

sample	Euclidean distance
physical mixture	3
active fiber 35% 1:6 CPM	3
active fiber 35% 1:8 CPM	5
placebo fiber 30%	9
pure E-EPO	11

Figure 16 shows a PCA biplot illustrating the distances from pure CPM. The dataset is projected onto a space relative to their distance from the two main principal components, which represent the axes of the map and correspond to the variance in the data.

PCA showed that the basic bitterness sensors AC0 and AN0 were responsible for principal component 1 (77.3% of variance). C00, the acidic bitterness sensor, was responsible for the second

DOI: 10.1021/acs.molpharmaceut.9b00159
Mol. Pharmaceutics 2019, 16, 2557−2568

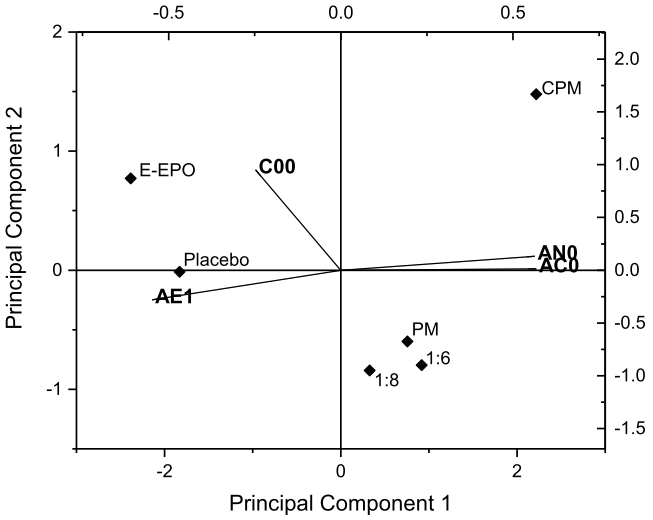

Figure 16. PCA biplot of 1:6 and 1:8 drug-loaded fibers compared to their physical mixtures, placebo fiber, pure E-EPO, and pure CPM.

principal component (22.4% of variance). This has a cumulative variance of 99.7%, which indicated that the change in data observed can be explained by the true change in taste as detected by the bitterness sensors. The upper right quadrant in the biplot shows pure CPM located in the direction of the AN0 and AC0 vectors, indicating its basic bitter taste. Pure E-EPO seems to elicit an acidic bitter response relative to the other samples; when formulated by electrospinning, the placebo fiber's C00, or acidic bitterness response, was decreased compared to pure E-EPO. The physical mixture and drug-loaded fibers are located neither in the basic bitterness nor in the acidic bitterness quadrants. This indicates that both the addition of the taste-masking polymer E-EPO and the process of electrospinning reduce the bitterness sensor response, relative to the other samples tested, concluding that the technique is capable of encapsulating bitter drugs.

4. CONCLUSIONS

To conclude, we have found using the electronic tasting system that electrospinning is a suitable taste-masking technology for the formulation of bitter pharmaceuticals. Although electrospinning is a simple and low-cost technique, it is affected by a number of parameters, and if not controlled properly, the outcomes can vary significantly. A DoE approach helped to accelerate the optimization process of electrospinning the E-EPO, saving time and resources.

The study has not only identified parameters for producing E-EPO fibers but has also developed an approach for the rational choice of electrospinning conditions, guiding the electrospinning of drug-loaded E-EPO fibers. Adding CPM to E-EPO changed both the conductivity and viscosity of the solutions and therefore yielded fibers with a different morphology. It was found that 35% w/v E-EPO fibers that have drug loads of 1:6 or higher yielded reproducible smooth nonbeaded fibers. Through solid-state characterization and thermal analysis of the fibers, it was shown that CPM is amorphously dispersed in the polymeric carrier E-EPO.

While maintaining the benefits of nanosizing a formulation, electrospinning is a promising taste-masking technology that if optimized efficiently through QbD principles can be utilized to formulate age-appropriate dosage forms. Using the results from this study, the drug-loaded fibers would be further formulated into an easy to swallow age-appropriate dosage form.

AUTHOR INFORMATION

Corresponding Author

*E-mail: duncan.craig@ucl.ac.uk. Phone: +44 (0) 207 753 5819. Fax: +44 (0) 207 753 5560.

ORCID

Hend E. Abdelhakim: 0000-0002-8344-2431

Mohan Edirisinghe: 0000-0001-8258-7914

Duncan Q. M. Craig: 0000-0003-1294-8993

Notes

The authors declare the following competing financial interest(s): This work was financially supported by the Medical Research Council, London, UK; iCASE Award No. 170156 and Pfizer Ltd, Sandwich, UK; Award No. 173803.

ACKNOWLEDGMENTS

This work was financially supported by the Medical Research Council, London, UK; iCASE award no. 170156 and Pfizer Ltd, Sandwich, UK; award no. 173803. The authors would like to thank Dr. Andrew Weston for his help with SEM imaging.

ABBREVIATIONS

CPM, chlorpheniramine maleate; DoE, design of experiment; E-EPO, Eudragit E PO

REFERENCES

(1) Qi, S.; Craig, D. Recent Developments in Micro- and Nanofabrication Techniques for the Preparation of Amorphous Pharmaceutical Dosage Forms. *Adv. Drug Deliv. Rev.* **2015**, *100*, 67−84.

(2) Brako, F.; Raimi-Abraham, B.; Mahalingam, S.; Craig, D. Q. M.; Edirisinghe, M. Making Nanofibres of Mucoadhesive Polymer Blends for Vaginal Therapies. *Eur. Polym. J.* **2015**, *70*, 186−196.

(3) Illangakoon, U. E.; Gill, H.; Shearman, G. C.; Parhizkar, M.; Mahalingam, S.; Chatterton, N. P.; Williams, G. R. Fast Dissolving Paracetamol/Caffeine Nanofibers Prepared by Electrospinning. *Int. J. Pharm.* **2014**, *477*, 369−379.

(4) Wu, Y.-H.; Yu, D.-G.; Li, X.-Y.; Diao, A.-H.; Illangakoon, U. E.; Williams, G. R. Fast-Dissolving Sweet Sedative Nanofiber Membranes. *J. Mater. Sci.* **2015**, *50*, 3604−3613.

(5) Samprasit, W.; Akkaramongkolporn, P.; Ngawhirunpat, T.; Rojanarata, T.; Kaomongkolgit, R.; Opanasopit, P. Fast Releasing Oral Electrospun PVP/CD Nanofiber Mats of Taste-Masked Meloxicam. *Int. J. Pharm.* **2015**, *487*, 213−222.

(6) Poller, B.; Strachan, C.; Broadbent, R.; Walker, G. F. A Minitablet Formulation Made from Electrospun Nanofibers. *Eur. J. Pharm. Biopharm.* **2017**, *114*, 213−220.

(7) Vrbata, P.; Berka, P.; Stránská, D.; Doležal, P.; Musilová, M.; Čižinská, L. Electrospun Drug Loaded Membranes for Sublingual Administration of Sumatriptan and Naproxen. *Int. J. Pharm.* **2013**, *457*, 168−176.

(8) Balogh, A.; Domokos, A.; Farkas, B.; Farkas, A.; Rapi, Z.; Kiss, D.; Nyiri, Z.; Eke, Z.; Szarka, G.; Örkényi, R.; Mátravölgyi, B.; Faigl, F.; Marosi, G.; Nagy, Z. K. Continuous end-to-end production of solid drug dosage forms: Coupling flow synthesis and formulation by electrospinning. *Chem. Eng. J.* **2018**, *350*, 290−299.

(9) Nagy, Z. K.; Balogh, A.; Demuth, B.; Pataki, H.; Vigh, T.; Szabo, B.; Molnar, K.; Schmidt, B. T.; Horak, P.; Marosi, G.; et al. High Speed Electrospinning for Scaled-up Production of Amorphous Solid Dispersion of Itraconazole. *Int. J. Pharm.* **2015**, *480*, 137.

(10) Jelvehgari, M.; Barghi, L.; Barghi, F. Preparation of Chlorpheniramine Maleate-Loaded Alginate/Chitosan Particulate Systems by the Ionic Gelation Method for Taste Masking. *Jundishapur J Nat Pharm Prod* **2014**, *9*, 39−48.

DOI: 10.1021/acs.molpharmaceut.9b00159
Mol. Pharmaceutics 2019, 16, 2557−2568

(11) Nollenberger, K.; Albers, J. Poly(Meth)Acrylate-Based Coatings. *Int. J. Pharm.* **2013**, *457*, 461−469.
(12) Guhmann, M.; Preis, M.; Gerber, F.; Pöllinger, N.; Breitkreutz, J.; Weitschies, W. Design, Development and in-Vitro Evaluation of Diclofenac Taste-Masked Orodispersible Tablet Formulations. *Drug Dev. Ind. Pharm.* **2015**, *41*, 540−551.
(13) Cooley, J. F. Apparatus for Electrically Dispersing Fluids. U.S. Patent 692,631, 1900, pp 1−6.
(14) Sarlak, N.; Nejad, M. A. F.; Shakhesi, S.; Shabani, K. Effects of Electrospinning Parameters on Titanium Dioxide Nanofibers Diameter and Morphology: An Investigation by Box-Wilson Central Composite Design (CCD). *Chem. Eng. J.* **2012**, *210*, 410−416.
(15) Nasouri, K.; Shoushtari, A. M.; Mojtahedi, M. R. M. Evaluation of Effective Electrospinning Parameters Controlling Polyvinylpyrrolidone Nanofibers Surface Morphology via Response Surface Methodology. *Fibers Polym.* **2015**, *16*, 1941−1954.
(16) Badawi, M. A.; El-Khordagui, L. K. A Quality by Design Approach to Optimization of Emulsions for Electrospinning Using Factorial and D-Optimal Designs. *Eur. J. Pharm. Sci.* **2014**, *58*, 44−54.
(17) Coles, S. R.; Jacobs, D. K.; Meredith, J. O.; Barker, G.; Clark, A. J.; Kirwan, K.; Stanger, J.; Tucker, N. A Design of Experiment Approach to Material Properties Optimization of Electrospun Nanofibres. *J. Appl. Polym. Sci.* **2010**, *117*, 2251−2257.
(18) Albetran, H.; Dong, Y.; Low, I. M. Characterization and Optimization of Electrospun TiO2/PVP Nanofibers Using Taguchi Design of Experiment Method. *J. Asian Ceram. Soc.* **2015**, *3*, 292−300.
(19) Khanlou, H. M.; Ang, B. C.; Talebian, S.; Barzani, M. M.; Silakhori, M.; Fauzi, H. Multi-Response Analysis in the Processing of Poly (Methyl Methacrylate) Nano-Fibres Membrane by Electrospinning Based on Response Surface Methodology: Fibre Diameter and Bead Formation. *Measurement* **2015**, *65*, 193−206.
(20) Ranjbar-Mohammadi, M.; Kargozar, S.; Bahrami, S. H.; Joghataei, M. Fabrication of Curcumin-Loaded Gum Tragacanth/Poly(Vinyl Alcohol) Nanofibers with Optimized Electrospinning Parameters. *J. Ind. Text.* **2017**, *46*, 1170−1192.
(21) Ruiter, F. A. A.; Alexander, C.; Rose, F. R. A. J.; Segal, J. I. A Design of Experiments Approach to Identify the Influencing Parameters That Determine Poly-D,L-Lactic Acid (PDLLA) Electrospun Scaffold Morphologies. *Biomed. Mater.* **2017**, *12*, 055009.
(22) Nasouri, K.; Bahrambeygi, H.; Rabbi, A.; Shoushtari, A. M.; Kaflou, A. Modeling and Optimization of Electrospun PAN Nanofiber Diameter Using Response Surface Methodology and Artificial Neural Networks. *J. Appl. Polym. Sci.* **2012**, *126*, 127−135.
(23) Nista, S. V. G.; Peres, L.; D'Ávila, M. A.; Schmidt, F. L.; Innocentini Mei, L. H. Nanostructured Membranes Based on Cellulose Acetate Obtained by Electrospinning, Part 1: Study of the Best Solvents and Conditions by Design of Experiments. *J. Appl. Polym. Sci.* **2012**, *126*, E70−E78.
(24) *International Conference on Harmonisation of Technical Requirements for Registration of Pharmaceuticals for Human Use*. 2009, No. August.
(25) Tahara, Y.; Toko, K. Electronic Tongues-a Review. *IEEE Sens. J.* **2013**, *13*, 3001−3011.
(26) Evonik Industries. *EUDRAGIT E PO EUDRAGIT E 12,5 EUDRAGIT E 100, EUDRAGIT E PO and EUDRAGIT E 12,5 Specification and Test Methods EUDRAGIT E PO EUDRAGIT E 12,5*. 2015, No. July, 1−6.
(27) Jones, B.; Nachtsheim, C. J. Effective Design-Based Model Selection for Definitive Screening Designs. *Technometrics* **2017**, *59*, 319−329.
(28) Chay, S. K.; Keating, A. V.; James, C.; Aliev, A. E.; Haider, S.; Craig, D. Q. M. Evaluation of the taste-masking effects of (2-hydroxypropyl)-*β*-cyclodextrin on ranitidine hydrochloride; a combined biosensor, spectroscopic and molecular modelling assessment. *RSC Adv.* **2018**, *8*, 3564−3573.
(29) Keating, A. V.; Soto, J.; Tuleu, C.; Forbes, C.; Zhao, M.; Craig, D. Q. M. Solid State Characterisation and Taste Masking Ef Fi Ciency Evaluation of Polymer Based Extrudates of Isoniazid for Paediatric Administration. *Int. J. Pharm.* **2018**, *536*, 536.
(30) Kong, L.; Ziegler, G. R. Molecular entanglement and electrospinnability of biopolymers. *J. Vis. Exp.* **2014**, *91*, e51933.
(31) Hong, X.; Edirisinghe, M.; Mahalingam, S. Beads, Beaded-Fibres and Fibres: Tailoring the Morphology of Poly(Caprolactone) Using Pressurised Gyration. *Mater. Sci. Eng., C* **2016**, *69*, 1373−1382.
(32) Husain, O.; Lau, W.; Edirisinghe, M.; Parhizkar, M. Investigating the particle to fibre transition threshold during electrohydrodynamic atomization of a polymer solution. *Mater. Sci. Eng., C* **2016**, *65*, 240−250.
(33) Koombhongse, S.; Liu, W.; Reneker, D. H. Flat Polymer Ribbons and Other Shapes by Electrospinning. *J. Polym. Sci., Part B: Polym. Phys.* **2001**, *39*, 2598−2606.
(34) De Vrieze, S.; Van Camp, T.; Nelvig, A.; Hagström, B.; Westbroek, P.; De Clerck, K. The Effect of Temperature and Humidity on Electrospinning. *J. Mater. Sci.* **2009**, *44*, 1357−1362.
(35) Williams, G. R.; Chatterton, N. P.; Nazir, T.; Yu, D.-G.; Zhu, L.-M.; Branford-White, C. J. Electrospun Nanofibers in Drug Delivery: Recent Developments and Perspectives. *Ther. Deliv.* **2012**, *3*, 515−533.
(36) Zuo, W.; Zhu, M.; Yang, W.; Yu, H.; Chen, Y.; Zhang, Y. Experimental Study on Relationship between Jet Instability and Formation of Beaded Fibers during Electrospinning. *Polym. Eng. Sci.* **2005**, *45*, 704−709.
(37) Williams, G. R.; Raimi-Abraham, B. T.; Lou, C. J. *Nanofibres in Drug Delivery*; 2018.
(38) Committee, J. F. *British National Formulary*, 73rd ed.; BMJ Group and Pharmaceutical Press: London, 2017.
(39) National Center for Biotechnology Information. PubChem Compound Database; CID=702, https://pubchem.ncbi.nlm.nih.gov/compound/702 (accessed Dec 6, 2017).
(40) Gupta, S. S.; Solanki, N.; Serajuddin, A. T. M. Investigation of Thermal and Viscoelastic Properties of Polymers Relevant to Hot Melt Extrusion, IV: Affinisol™ HPMC HME Polymers. *AAPS PharmSciTech* **2016**, *17*, 148−157.
(41) PubChem Chlopheniramine https://pubchem.ncbi.nlm.nih.gov/compound/chlorpheniramine#section=Solubility (accessed Aug 15, 2017).
(42) Payab, S.; Jafari-Aghdam, N.; Barzegar-Jalali, M.; Mohammadi, G.; Lotfipour, F.; Gholikhani, T.; Adibkia, K. Preparation and physicochemical characterization of the azithromycin-Eudragit RS100 nanobeads and nanofibers using electrospinning method. *J. Drug Deliv. Sci. Technol.* **2014**, *24*, 585−590.
(43) Rahman, Z.; Zidan, A. S.; Khan, S. R.; Reddy, I. K.; Khan, M. A. Cholorpheniramine Tannate Complexes: Physicochemical, Chemometric, and Taste Masking Evaluation. *Int. J. Pharm.* **2012**, *436*, 582−592.

DOI: 10.1021/acs.molpharmaceut.9b00159
Mol. Pharmaceutics 2019, 16, 2557−2568